Electronic Supplementary Material (ESI) for Dalton Transactions.

Electronic Supporting Information

for the

Manuscript Entitled

Detection of anticoagulant drug warfarin by palladium complexes

Pramod Kumar, Vijay Kumar and Rajeev Gupta*

Department of Chemistry, University of Delhi, Delhi 110 007 (India)

Index

1. Experimental Section

Materials. All reagents and metal salts were commercial available and were used without further purifications. HPLC grade solvents were used for the UV-visible and fluorescence spectral measurements. Warfarin sodium (Na^+WR^-) was obtained from the TCI Chemicals and used as received. In addition, commercial drug WARF was also used that provided nearly identical results as that of Na^+WR^- obtained from the TCI Chemicals. All stock solutions (1 mM) of palladium complexes and anticoagulant drug Na^+WR^- were prepared in CH_3CN and/or aqueous HEPES buffer (10 mM, pH = 7.4).

2. Synthesis. Ligands H_2L^1-H_2L^4 were synthesized according to the reported procedure.[1,2] The palladium complexes **1** and **3** were synthesized according to the literature report.[3]

Complex 2. Ligand H_2L^2 (0.10 g, 0.224 mmol) was dissolved in CH_3CN (5 mL) and a solution of $Pd(CH_3COO)_2$ in 2 mL CH_3CN (0.050 g, 0.224 mmol)was added drop-wise. The reaction mixture was stirred for 2 h at ambient temperature during which a pale yellow colored compound was precipitated. This product was filtered, washed with MeOH and dried under vacuum. Yellow crystals were obtained by the slow evaporation of a CH_3CN solution of the product within three days. Yield: 0.108 g (82%). Anal. Calc. for $C_{31}H_{24}N_4O_2Pd$: C, 63.00; H, 4.09; N, 9.48. Found: C, 63.06; H, 4.12; N, 9.53. FTIR spectrum (Zn-Se ATR, cm^{-1}): 2327- 2297 (CH_3CN), 1601 (C=O), 1374. UV/Vis (CH_3CN): λ_{max} (ε, M^{-1} cm^{-1}) = 216 (125140), 335 (20500). ^1H NMR spectrum (400 MHz, DMSO-d_6): δ = 8.23 (t, J = 6.88 Hz, 1H), 8.09 (d, J = 6.87 Hz, 2H), 7.90 (d, J = 7.64 Hz, 2H), 7.77-7.71 (m, 6H), 7.55-7.45 (m, 6H), 4.74 (s, 4H), 2.06 (s, CH_3CN). ^{13}C NMR spectrum (400 MHz, DMSO-d^6): 170.40, 133.50, 131.05, 128.86, 126.82, 126.28, 125.85, 124.85, 123.15.

Complex 4. This compound was synthesized similarly as mentioned for complex **2** using following chemical: H_2L^4 (0.10 g, 0.193 mmol) and $Pd(CH_3COO)_2$ (0.043 g, 0.193 mmol). Orange-red crystals were obtained by the slow evaporation of a CH_3CN solution of the product within 2 – 3 d. Yield: 0.110 g (86%). Anal. Calc. for $C_{37}H_{24}N_4O_2Pd$: C, 67.02; H, 3.65; N, 8.45. Found: C, 67.18; H, 3.59; N, 8.38. FTIR spectrum (cm^{-1}): 2332-2305 (CH_3CN), 1623 (C=O). UV/Vis (CH_3CN): λ_{max} (ε, M^{-1} cm^{-1}) = 254 (93850), 324 (24650), 374 (11450), 394 (8090). ^1H

NMR spectrum (400 MHz, DMSO-d^6): δ = 8.44 (d, *J* = 10.1 Hz, 4H), 8.33 (t, *J* = 7.8 Hz, 1H), 8.03-7.91 (m, 6H), 7.88-7.77 (m, 4H), 7.51-7.38 (m, 6H), 2.03 (s, CH_3CN). ^{13}C NMR spectrum (400 MHz, DMSO-d^6): 168.79, 152.59, 144.01, 132.10, 131.92, 131.16, 129.65, 128.61, 128.32, 128.19, 127.92, 126.29, 126.22, 126.04, 125.58, 125.42, 123.20.

3. Physical Measurements

Elemental analysis data were obtained from Elementar Analysen Systeme GmbH Vario EL-III instrument. The ^{1}H and ^{13}C NMR spectra were recorded with a JEOL 400 MHz instrument. The FTIR spectra (Zn–Se ATR) were recorded with a Perkin-Elmer Spectrum-Two spectrometer. The absorption spectra were recorded with a Perkin-Elmer Lambda-25 spectrophotometer. Fluorescence spectral studies were performed with a Cary Eclipse fluorescence spectrophotometer. Time-resolved fluorescence spectra were recorded using a picosecond Fluorimeter from Horiba JobinYvon (FluoroHub). All UV-visible and fluorescence spectra were recorded with a 1.0 cm path length cuvette. The circular dichroism (CD) spectral measurements were recorded on Jasco spectropolarimeter (J815, Japan) equipped with peltier accessory. The spectrometer was sufficiently purged with 99.9% dry nitrogen before the CD measurements. The spectra were collected at a scan rate speed of 50 nm min^{-1} with a response time of 1 s. Each spectrum was baseline corrected and the final plot was taken as an average of three accumulated plots in the range of 200 nm–300 nm. ESI$^+$-MS mass spectra were obtained with a Q-TOF LC/MS Agilent mass spectrometer whereas ESI$^-$-MS mass spectra was recorded with Bruker micrOTOF^{TM}-Q II. Docking studies were performed using the Hex 6 software.

4. X-ray Crystallography

Single crystals suitable for the X-ray diffraction studies were grown by the slow evaporation of a CH_3CN solution of complex **4**. The intensity data were collected at 298 K with an Oxford XCalibur CCD diffractometer equipped with graphite monochromatic Mo-*K*α radiation (*λ* = 0.71073 Å).[4] Data reduction was performed with the CrysAllisPro program (Oxford Diffraction ver. 171.34.40).[4] The structure was solved by direct methods using SIR-92 program[5] and refined on F^2 using all data by full matrix least-squares procedures with SHELXL-2014/7[6]The hydrogen atoms were placed at the calculated positions and included in the last cycles of the refinement. All calculations were done using the WinGX software package.[7] Crystallographic data collection

and structure solution parameters are summarized in Table S1. CCDC-1522061 contains the supplementary crystallographic data for this paper. This data can be obtained free of charge from The Cambridge Crystallographic Data Center via www.ccdc.cam.uk/data_request/cif.

5. Determination of Stern-Volmer Constant (K_{SV}) and Binding Constant (K_b)

Stern-Volmer constant (K_{SV}) were computed by the Stern–Volmer equation (1)[8] where, I_0 and I are the emission in the absence and in the presence of complexes **1-4** used as the quencher (Q).

The binding constant (K_b) was computed by the Benesi-Hildebrand equation (2)[9] where I, I_0 and I_{min} are the emission intensities of Na^+WR^- in presence of complexes, in absence of complexes and minimum fluorescence intensity in presence of complexes, respectively. K_b value was obtained by the ratio of intercept and slope in $1/(I-I_0)$ vs. $1/[\mathbf{1\text{-}4}]$ plots.

$$I_0/I = 1 + K_{SV}[\mathbf{1\text{-}4}] \qquad (1)$$

$$1/(I-I_0) = 1/\{K_b(I_0 - I_{min})[\mathbf{1\text{-}4}]\} + 1/(I_0 - I_{min}) \qquad (2)$$

6. Determination of Detection Limit

From fluorescence spectral titration: The detection limit was calculated according to equation (3)[10] where, k is the slope of a plot of emission of Na^+WR^- versus concentration of complexes **1-4** and σ is the standard deviation of ten blank replicate fluorescence measurements of Na^+WR^-.

$$\text{Detection limit: } 3\sigma/k \qquad (3)$$

From UV-visible spectral titration: The detection limit for the detection of Na^+WR^- by Pd(II) complexes **3** and **4** in CH_3CN and in HEPES buffer was calculated according to equation (4)[11] where, k' is the slope of a plot of absorbance of Pd(II) complexes **3** or **4** versus concentration of Na^+WR^- and σ' is the standard deviation of ten blank replicate UV-visible measurements of complexes.

$$\text{Detection limit: } 3\sigma'/k' \qquad (4)$$

7. References

1. P. Kumar, V. Kumar and R. Gupta, *RSC Adv.*, 2015, **5**, 97874.
2. A. N. Dwyer, M. C. Grossel and P. N. Horton, *Supramol. Chem.*, 2004, **16**, 405.
3. Q.-Q. Wang, R. A. Begum and V. W. Day, *J. Am. Chem. Soc.*, 2013, **135**, 17193.
4. CrysAlisPro, v. 1.171.33.49b, Oxford Diffraction Ltd., 2009.
5. A. Altomare, G. Cascarano, C. Giacovazzo and A. Guagliardi, *J. Appl. Crystallogr.*, 1993, **26**, 343-350.
6. Sheldrick,G. M.*SHELXL-2014/7*: *Program for the solution of crystal structures*, University of Gottingen, Gottingen, Germany, 2014.
7. Farrugia, L. J. WinGX, v. 1.70, An Integrated System of Windows Programs for the Solution, Refinement and Analysis of Single- Crystal X-ray Diffraction Data, Department of Chemistry, University of Glasgow, 2003.
8. A. Ganguly, B. K. Paul, S.Ghosh, S. Kar and N.Guchhait, Analyst, 2013, **138**, 6532.
9. H. A. Benesi and J. H. Hildebrand, *J. Am. Chem. Soc.*, 1949, **71**, 2703.
10. A. Senthilvelan, I. Ho, K. Chang, G. Lee, Y. Liu and W. Chung, *Chem.–Eur. J.*, 2009, **15**, 6152.
11. S. Goswami, K. Aich, S. Das, A. K. Das, A. Mannaa and S. Halder, *Analyst,* 2013, **138**, 1903.

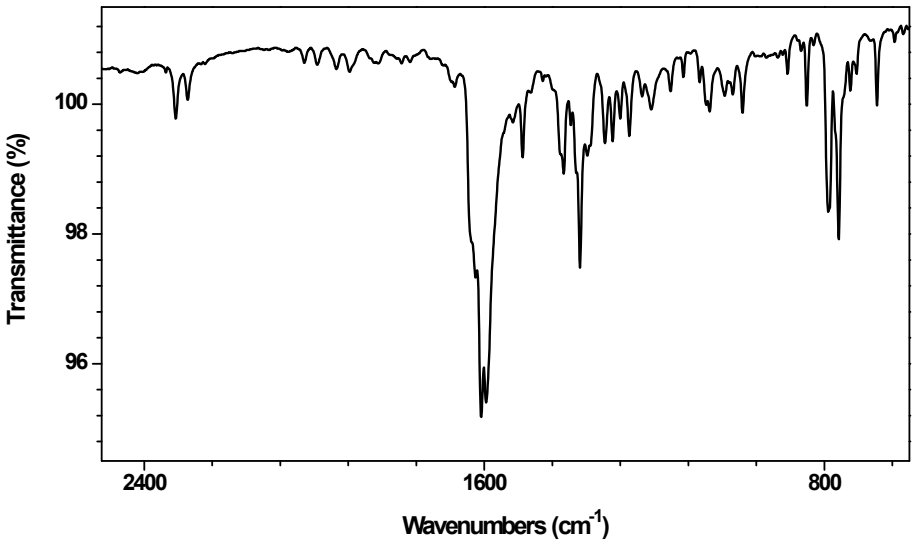

Figure S1. FTIR spectrum of complex **2**.

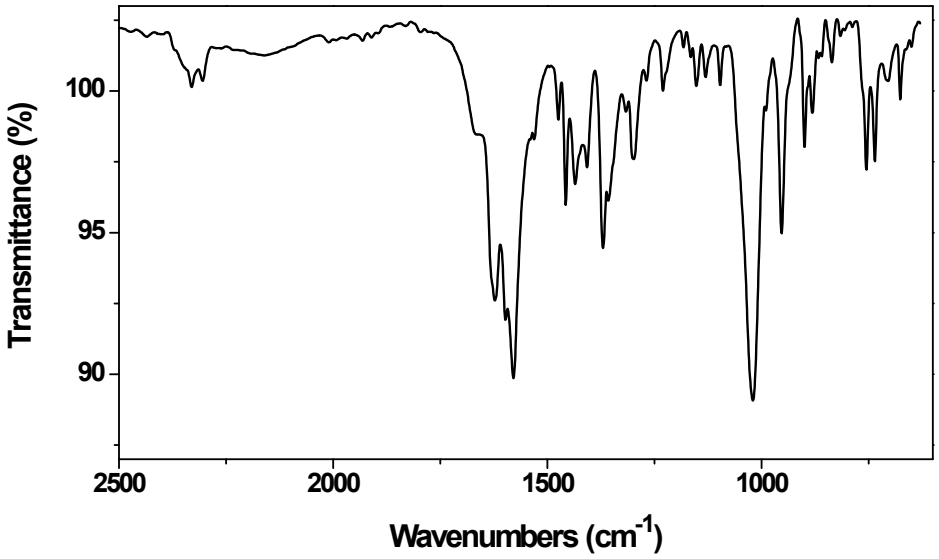

Figure S2. FTIR spectrum of complex **4**.

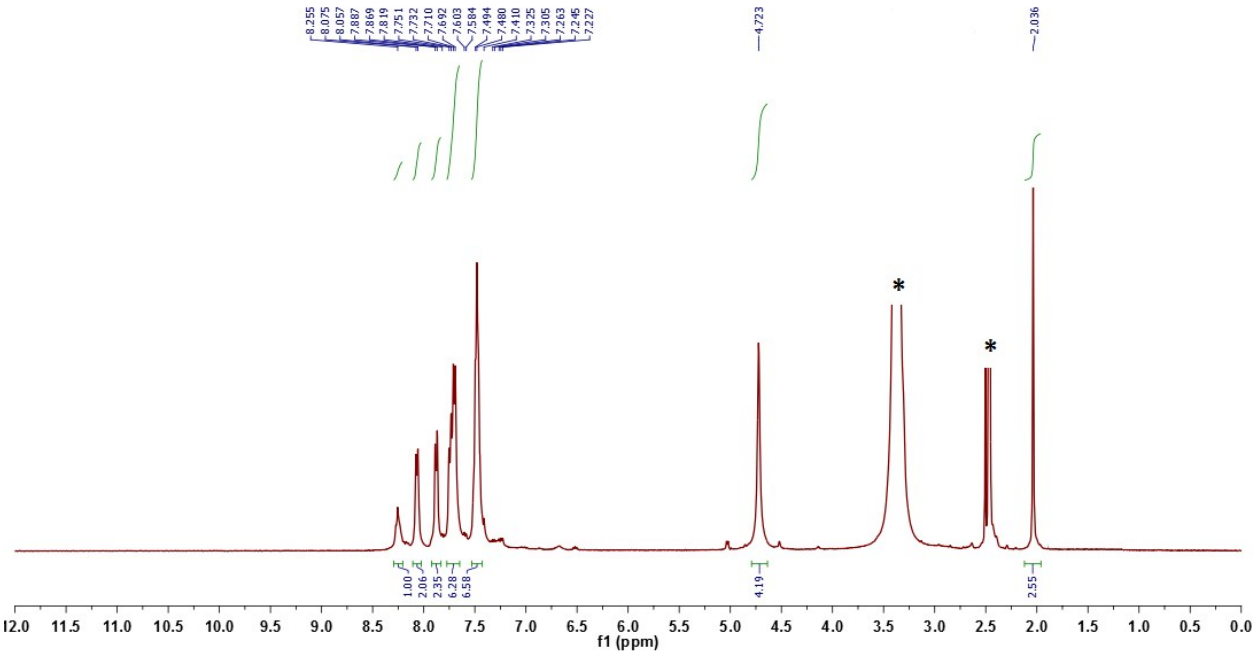

Figure S3. ^{1}H NMR spectrum of complex **2** in DMSO-d_6 where * represents the residual solvent and/or adventitious water peak(s).

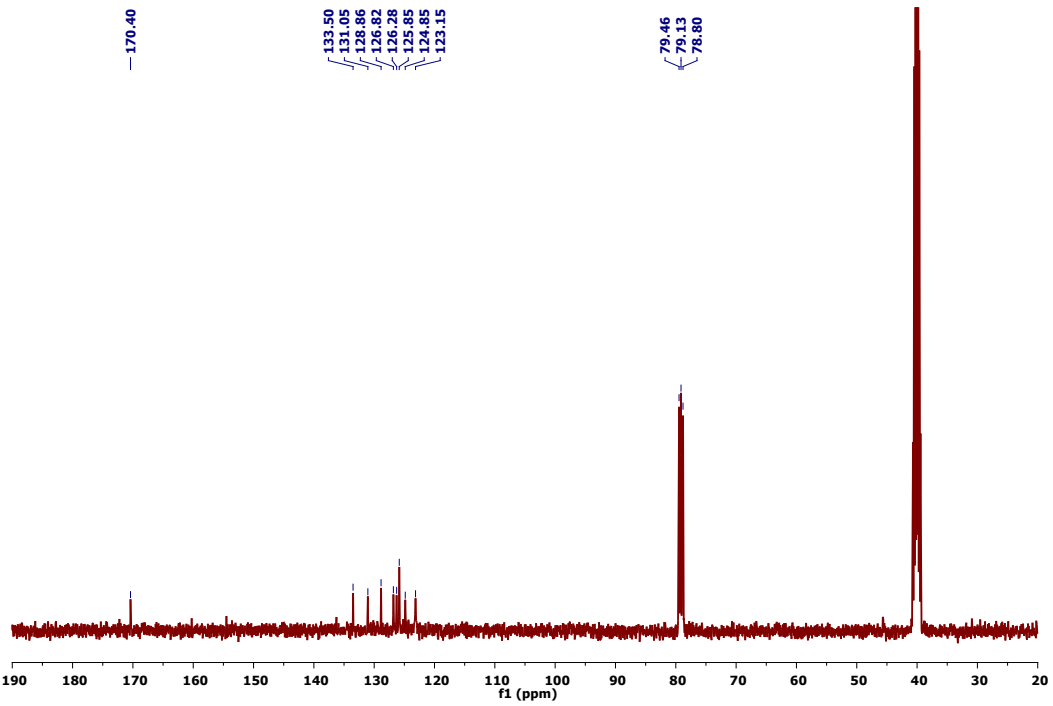

Figure S4. ^{13}C NMR spectrum of complex **2** in DMSO-d_6.

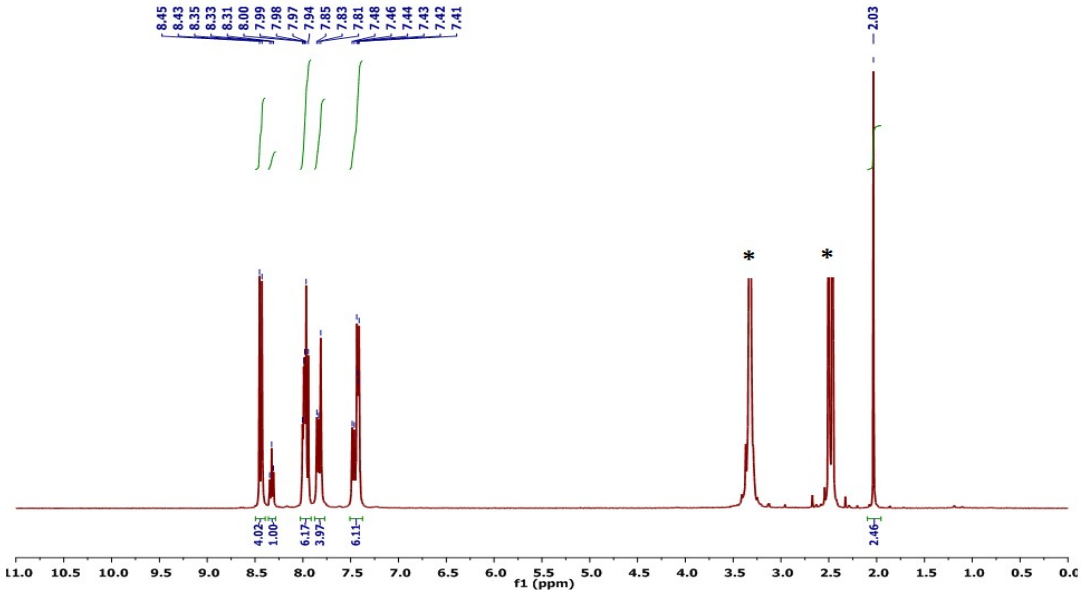

Figure S5. ^{1}H NMR spectrum of complex **4** in DMSO-d_6 where * represents the residual solvent and/or adventitious water peak(s).

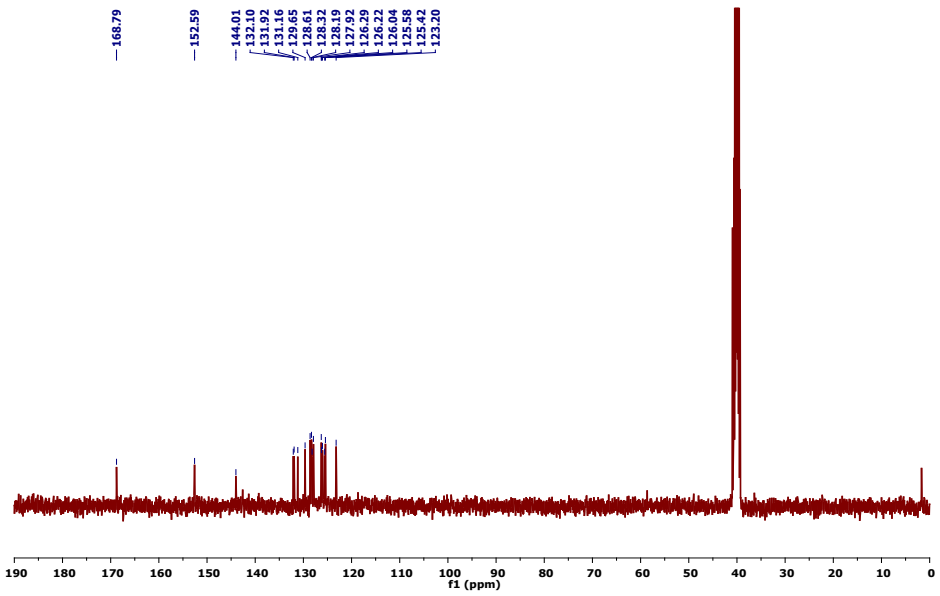

Figure S6. ^{13}C NMR spectrum of complex **4** in DMSO-d_6.

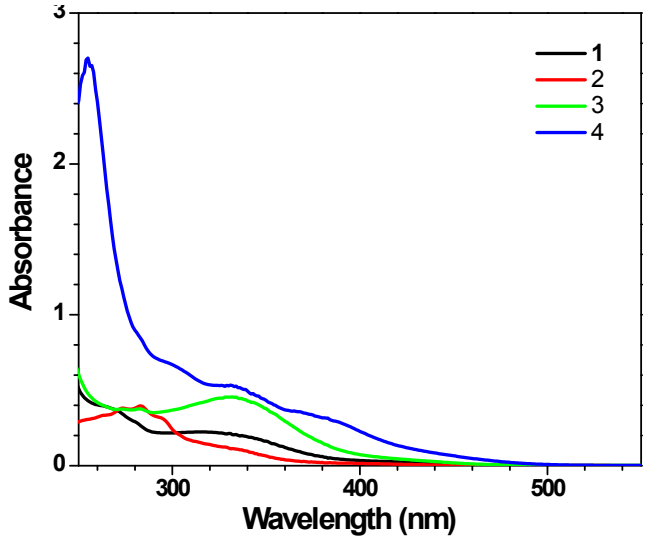

Figure S7. UV-visible spectra of complexes **1-4** recorded in CH_3CN (20 μM).

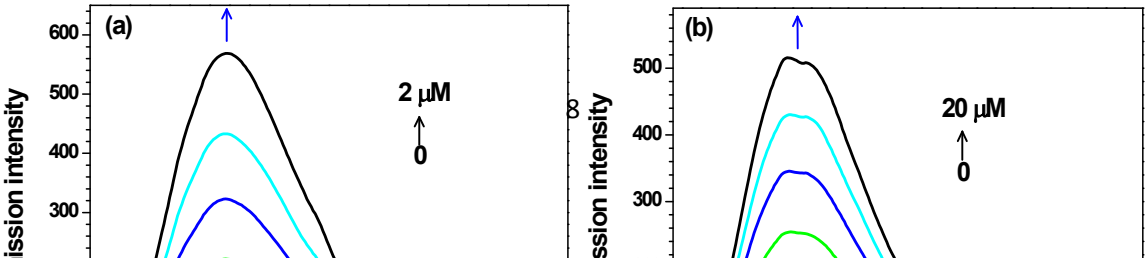

Figure S8. Change in emission intensity of Na^+WR^- in CH_3CN (λ_{ex} = 320 nm) and in HEPES buffer (10 mM, pH = 7.4) (λ_{ex} = 310 nm).

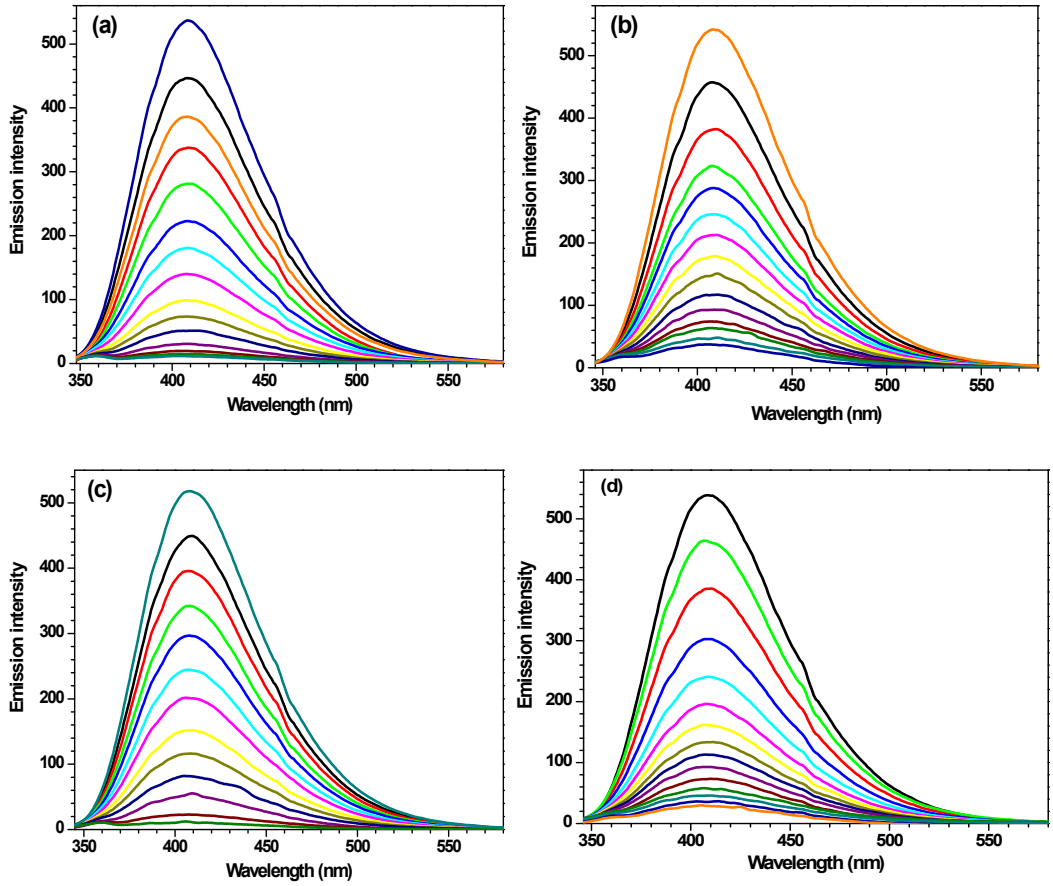

Figure S9. Emission spectra of Na^+WR^- (2 μM) and after its interaction with Pd(II) complexes (0-2.8 μM) (a) **1**; (b) **2**; (c) **3** and (d) **4** in CH_3CN (λ_{ex} = 320 nm).

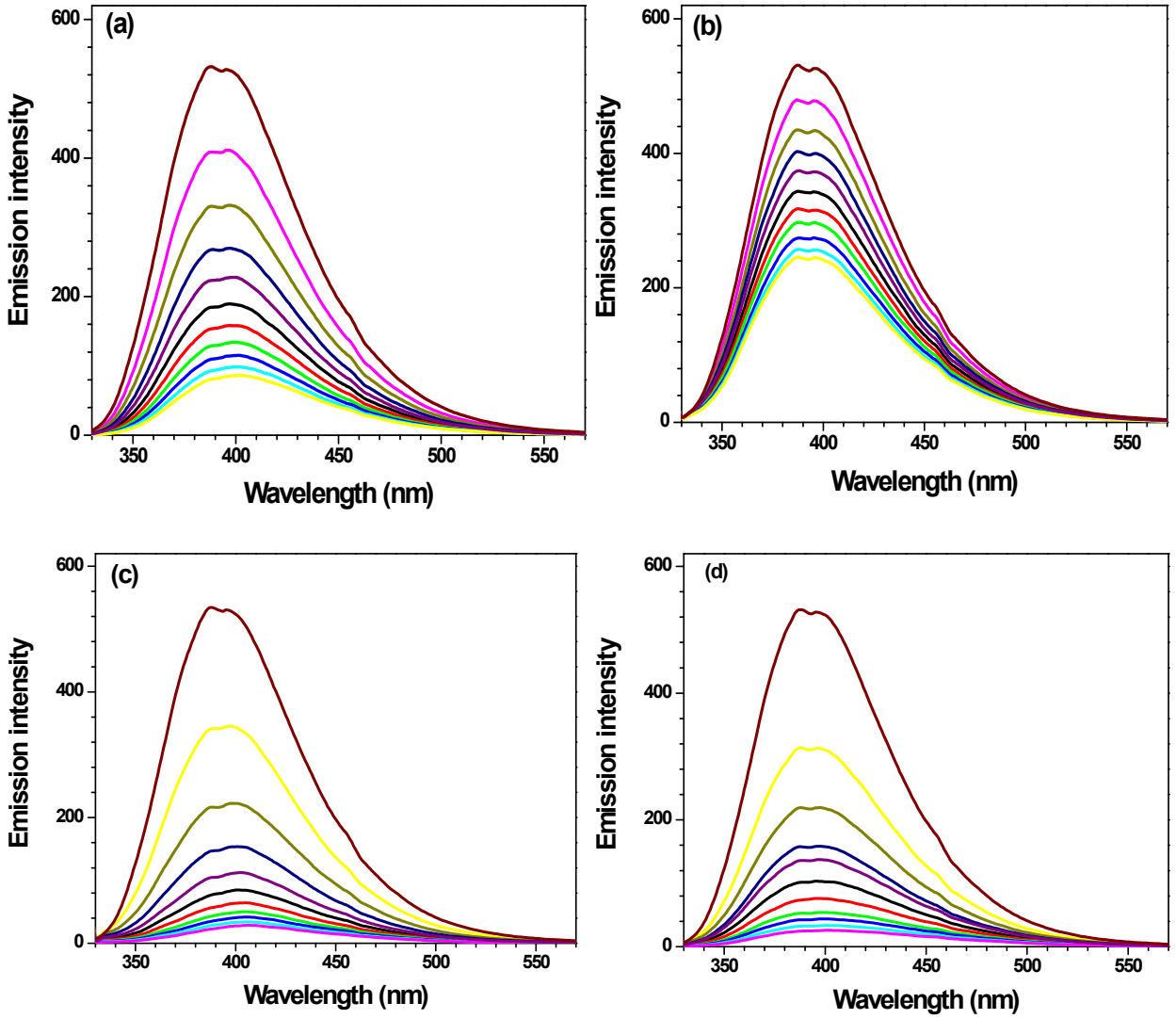

Figure S10. Emission spectra of $Na^{+}WR^{-}$ (20 μM) and after its interaction with Pd(II) complexes (0-200 μM) (a) **1**; (b) **2**; (c) **3** and (d) **4** in HEPES buffer (10 mM, pH = 7.4) (λ_{ex} = 310 nm).

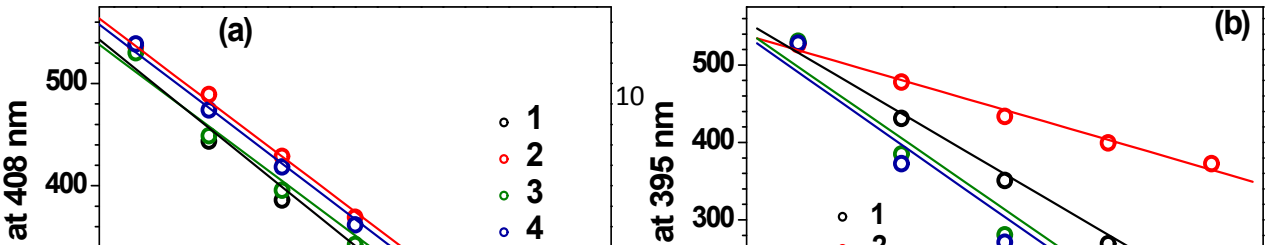

Figure S11. Determination of detection limit of (**a**) Na^+WR^- (2 μM) with Pd(II) complexes **1-4** (concentration was linear from 0 –1.2 μM) in CH_3CN. (**b**) Na^+WR^- (20 μM) towards Pd(II) complexes **1-4** (concentration was linear from 0 –100 μM) in HEPES buffer (10 mM, pH = 7.4).

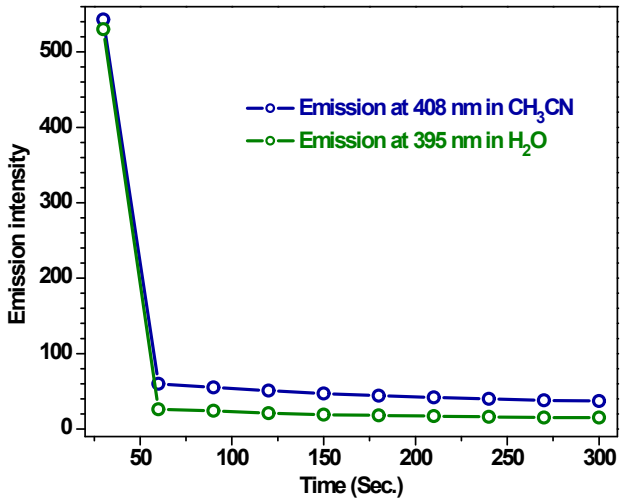

Figure S12. Time-dependent emission intensity of Na^+WR^- (2 μM in CH_3CN, 20 μM in buffer) in CH_3CN and in HEPES buffer (10 mM, pH = 7.4) as a function of concentration of complex **4**. Points at 0 second represent the emission of only Na^+WR^- without the addition of complex **4**.

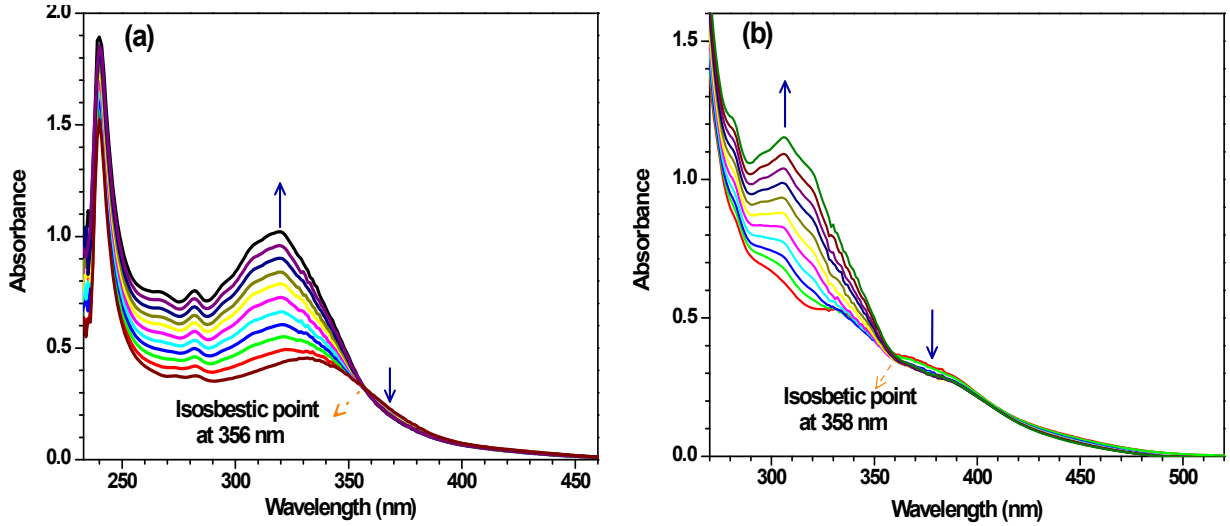

Figure S13. Change in absorbance of Pd(II) complexes (a) **3** (20 μM) and (b) **4** (20 μM) in presence of $Na^{+}WR^{-}$ (0 – 50 μM) in CH_3CN.

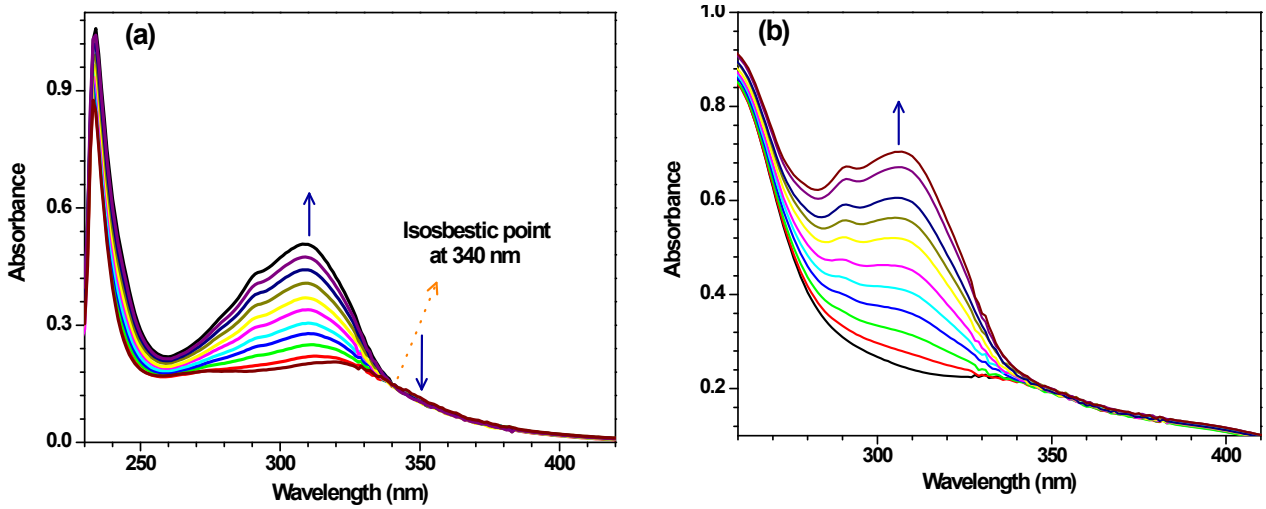

Figure S14. Change in absorbance of Pd(II) complexes (a) **3** (10 μM) and (b) **4** (10 μM) in presence of $Na^{+}WR^{-}$ (0 - 25 μM) in HEPES buffer (10 mM, pH = 7.4).

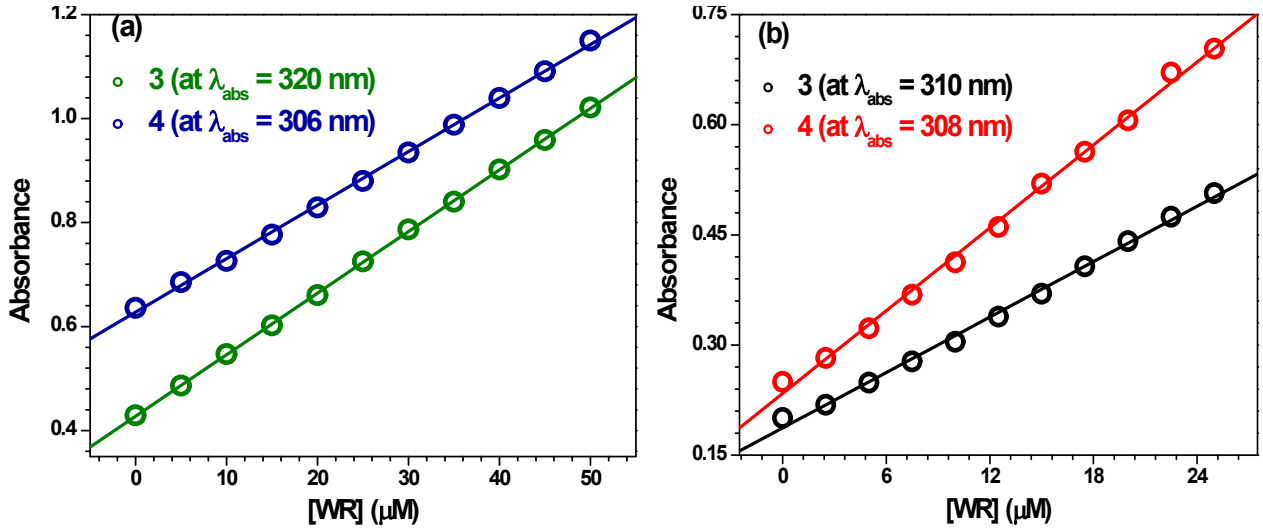

Figure S15. Determination of detection limit of $Na^{+}WR^{-}$ by UV-visible titration of (**a**) Pd(II) complexes **3** (20 μM) and **4** (20 μM) by $Na^{+}WR^{-}$ (0– 50 μM) in CH_3CN. (**b**) Pd(II) complexes **3**

(10 μM) and **4** (10 μM) by Na^+WR^- (0– 25 μM) in HEPES buffer (10 mM, pH = 7.4).

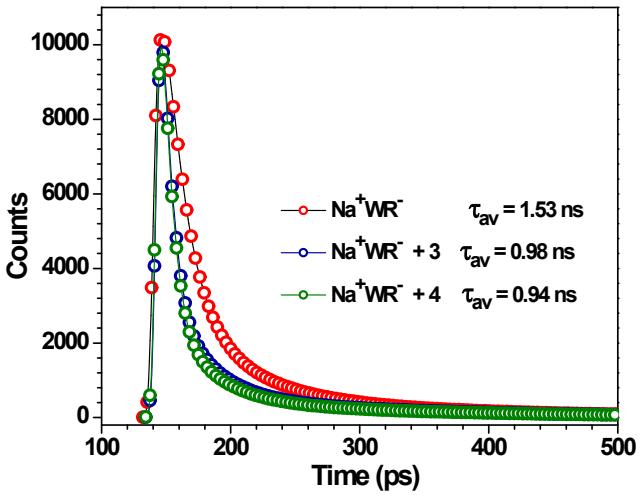

Figure S16. Lifetime profile of Na^+WR^- in absence and presence of Pd(II) complexes **3** and **4** (5 equiv.) in CH_3CN (λ_{ex} = 280 nm, λ_{em} = 395 nm).

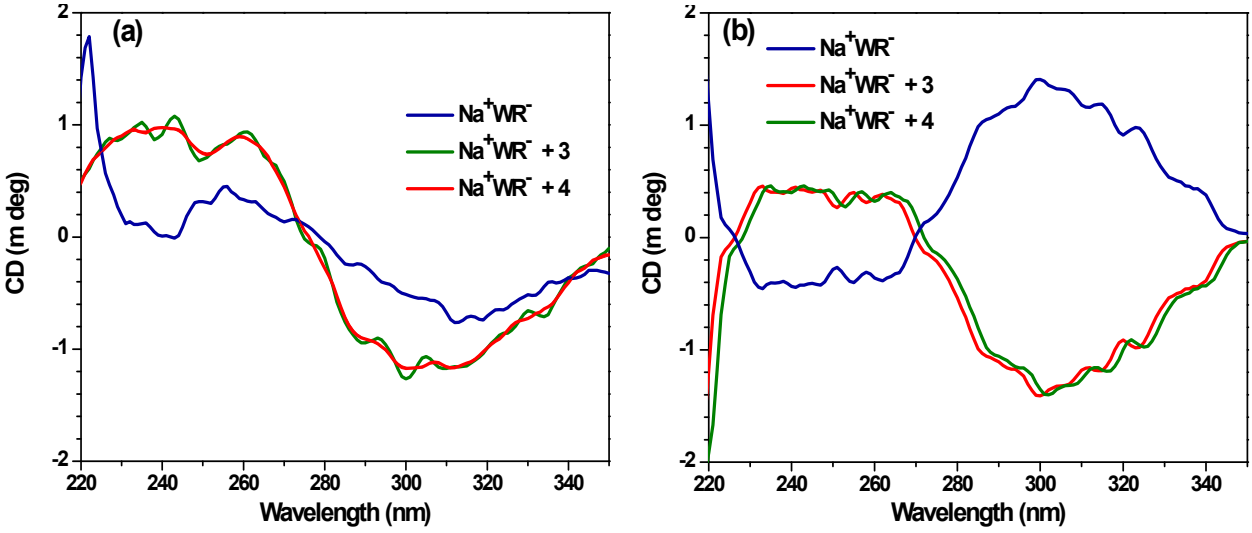

Figure S17. (a) Circular dichroism spectra of Na^+WR^- (100 μM) in absence and presence of Pd(II) complexes **3** and **4** (5 equiv.) in CH_3CN. (b) Circular dichroism spectra of Na^+WR^- (35

μM) in absence and presence of complexes **3** and **4** (10 equiv.) in HEPES buffer (10 mM, pH = 7.4).

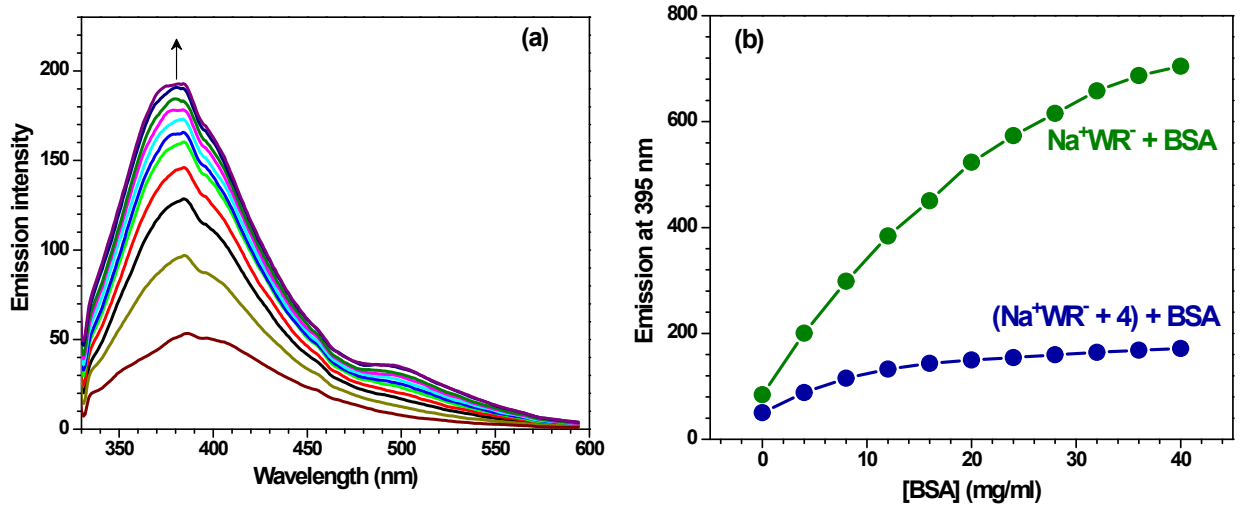

Figure S18. (a) Change in emission intensity of Na^+WR^-+complex **4** (2 μM, 20 μM) in presence of BSA (0–40 mg/mL). (b) Change in emission intensity of Na^+WR^- (2 μM) in presence of BSA (0–40 mg/mL) and Na^+WR^-+complex **4** (2 μM, 20 μM) in presence of BSA (0–40 mg/mL) in HEPES buffer (10 mM, pH = 7.4).

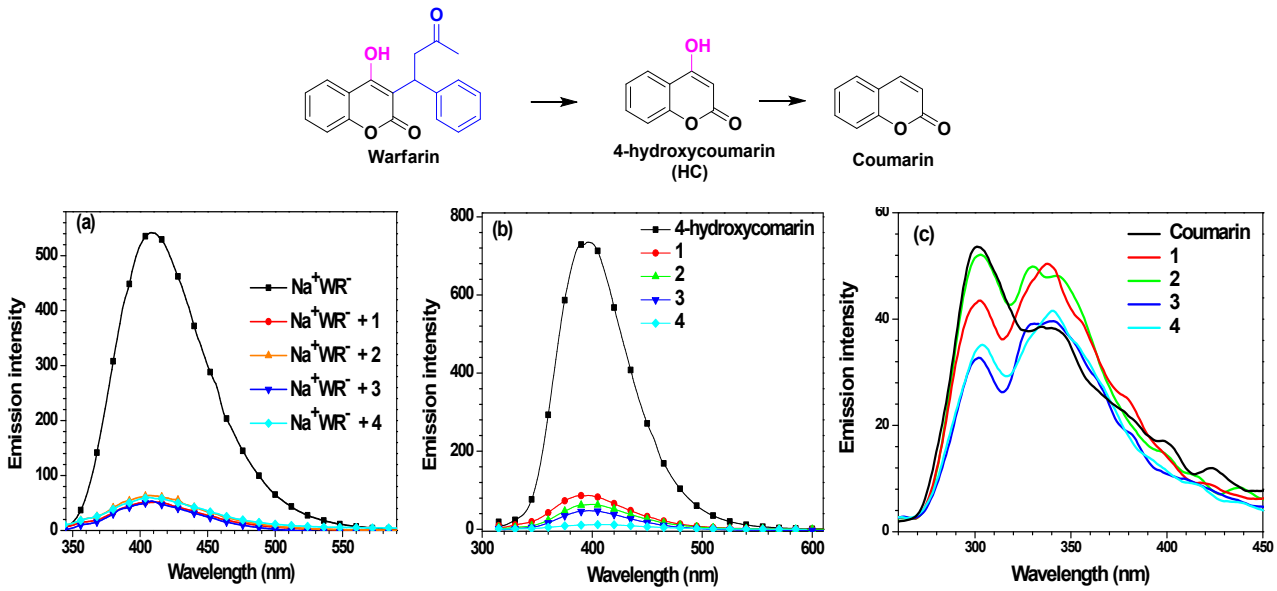

Figure S19 (**a**) Emission spectra of $Na^{+}WR^{-}$ (2 μM) and after its interaction with complexes **1-4** (2 μM) in CH_3CN. (**b**) Emission spectra of 4-hydroxycoumarin (50 μM) in absence and in presence of complexes **1-4** (50 μM) in CH_3CN (λ_{ex} = 300 nm). **(c)** Emission spectra of coumarin (10 μM) in absence and in presence of complexes **1-4** (10 μM) in CH_3CN (λ_{ex} = 225 nm).

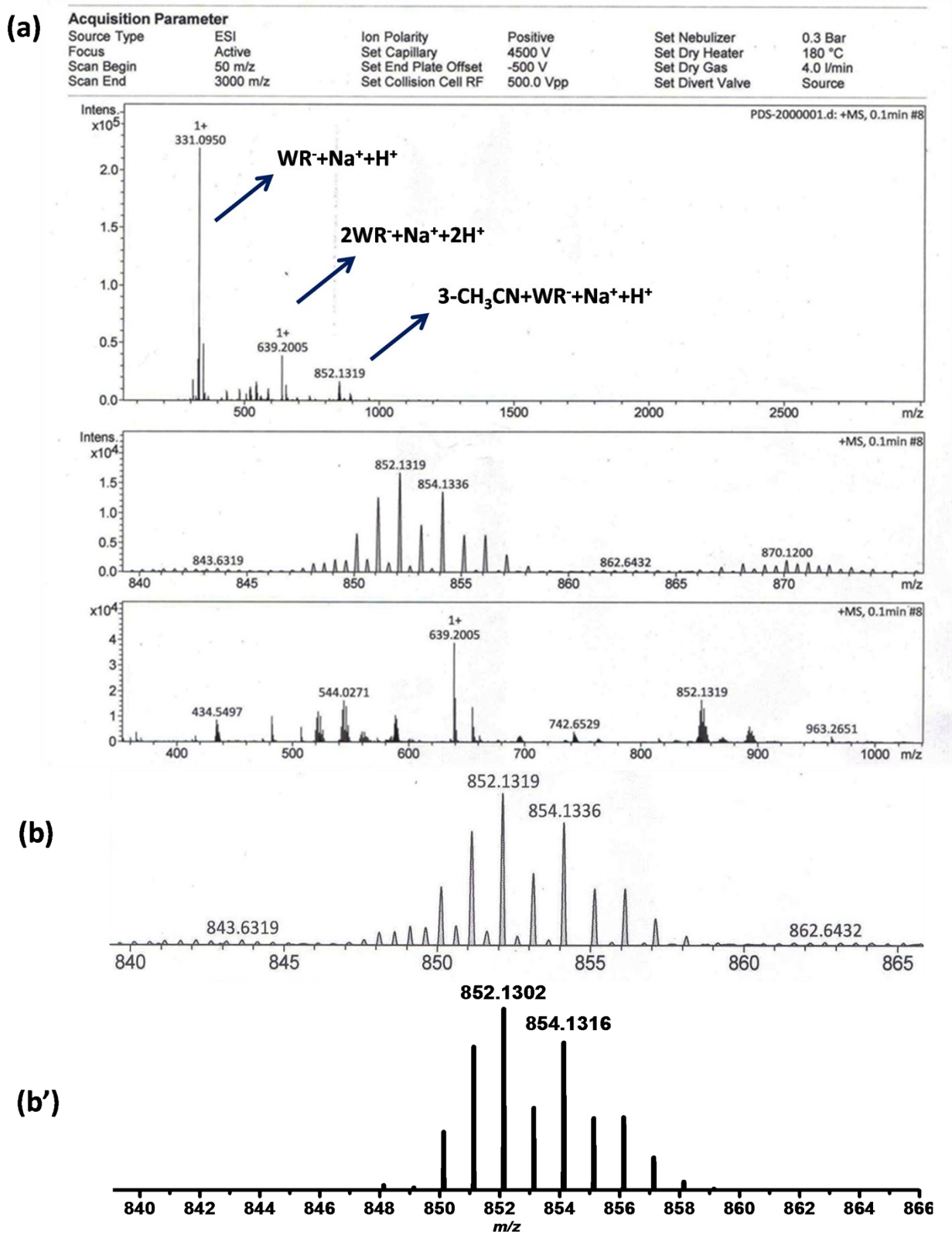

Figure S20. (a) ESI$^+$-MS spectra of a mixture of complex **3** and Na^+WR^- in CH_3CN. b and b' are isotopic patterns at *m/z* = 852 and its simulation, respectively.

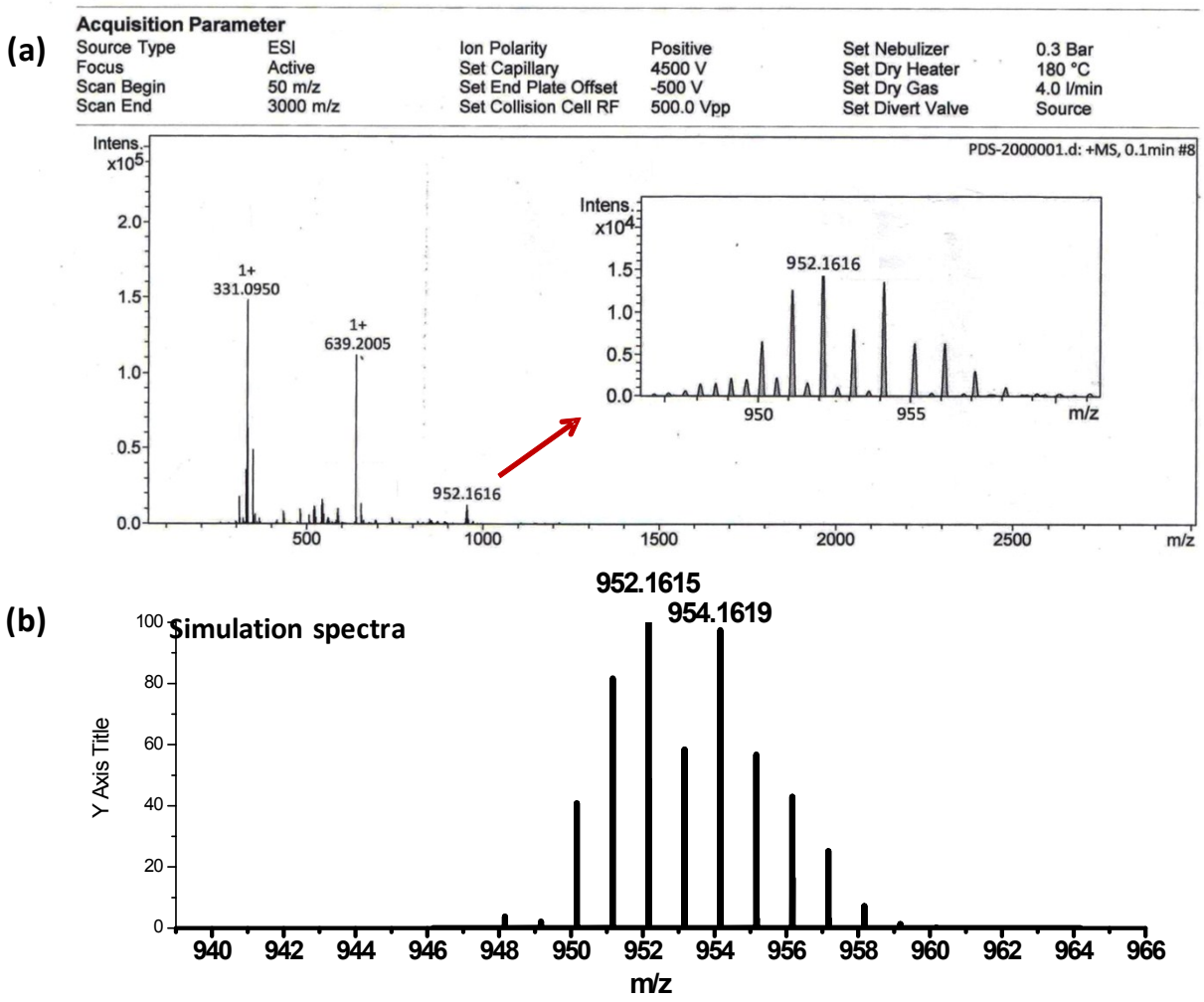

Figure S21. (a) ESI^{+}-MS spectrum of a mixture of complex **4** and $Na^{+}WR^{-}$ in CH_3CN. (**b**) The corresponding simulation pattern.

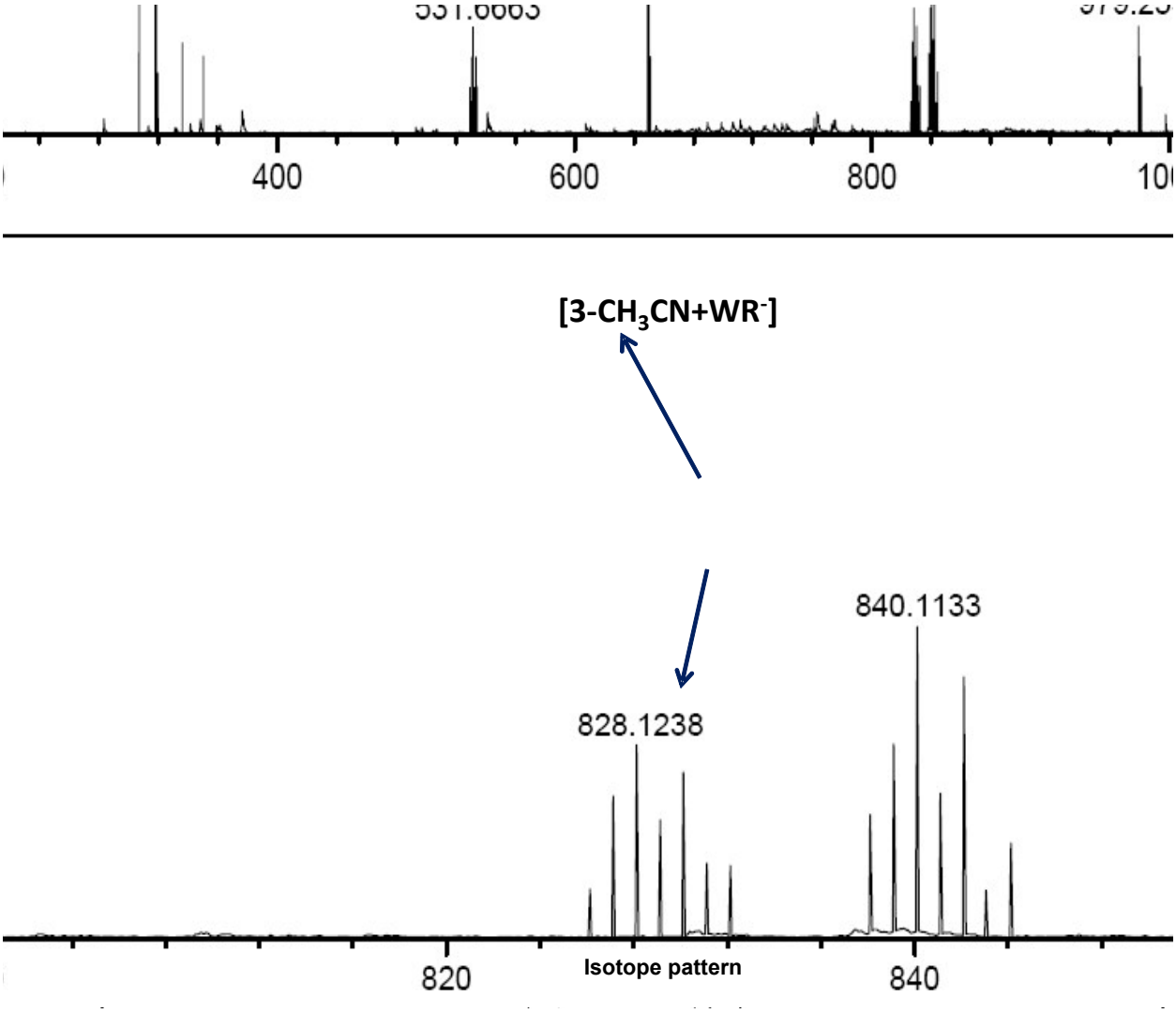

Figure S22. ESI$^-$-MS spectrum of a mixture of complex **3** and Na^+WR^- in CH_3CN along with its isotope distribution pattern and the corresponding simulated pattern for [**3**–CH_3CN+WR^-]$^-$.

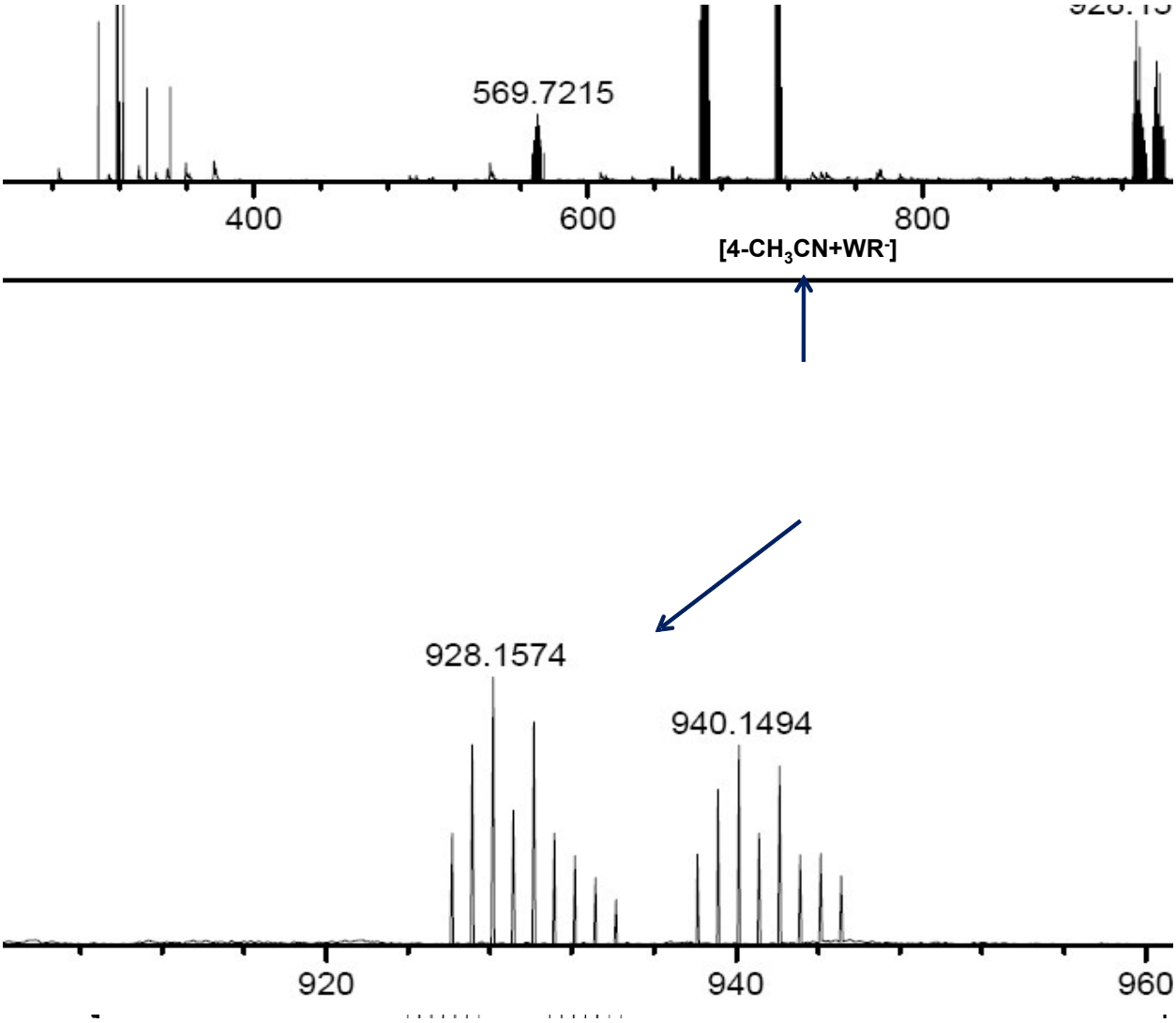

Figure S23. ESI^{-}-MS spectrum of a mixture of complex **4** and $Na^{+}WR^{-}$ in CH_3CN along with its isotope distribution pattern and the corresponding simulated pattern for $[\mathbf{4}–CH_3CN+WR^{-}]^{-}$.

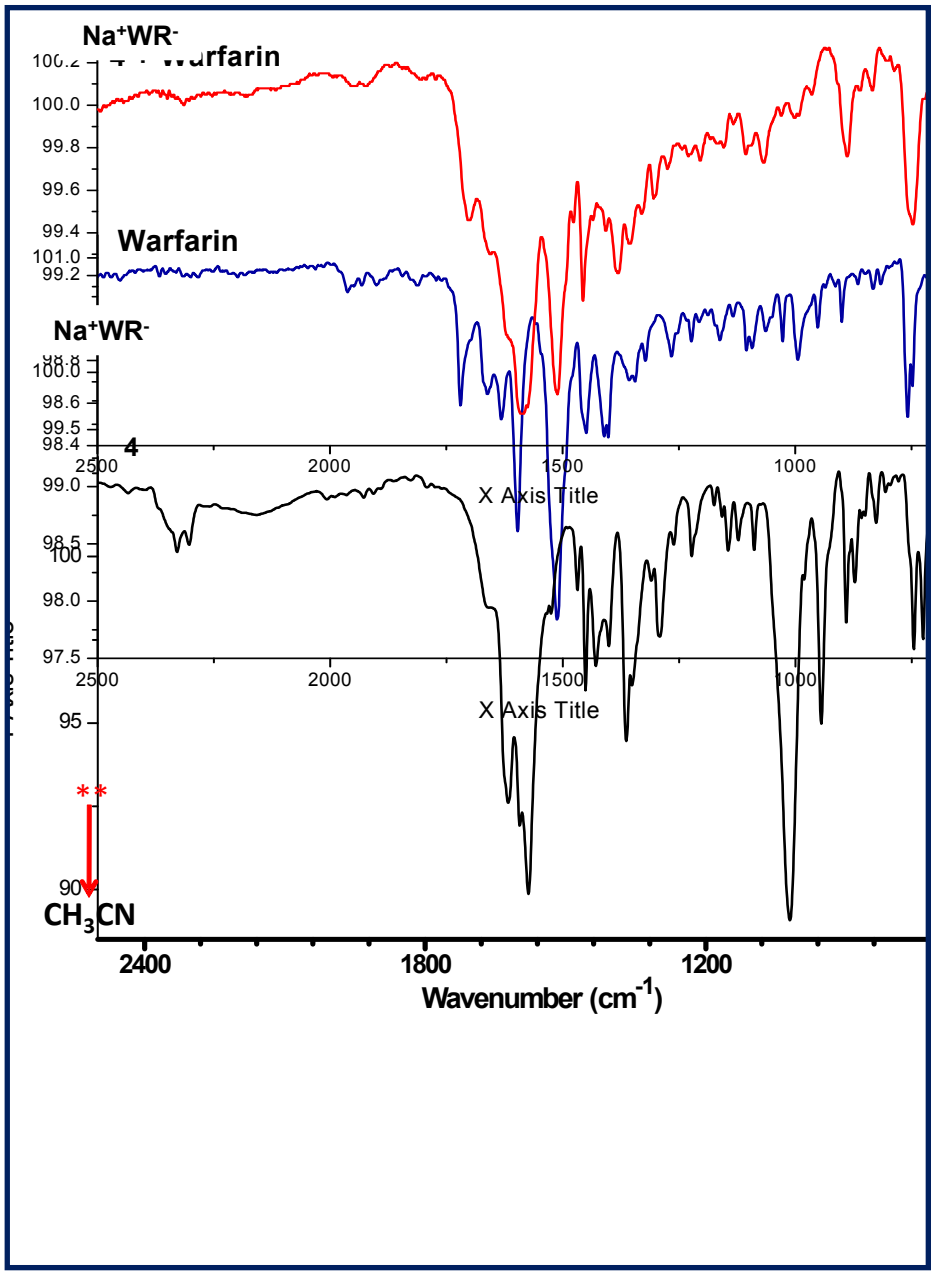

Figure S24. FTIR spectra of complex **4**, $Na^{+}WR^{-}$ and the isolated product from the reaction between complex **4** and $Na^{+}WR^{-}$.

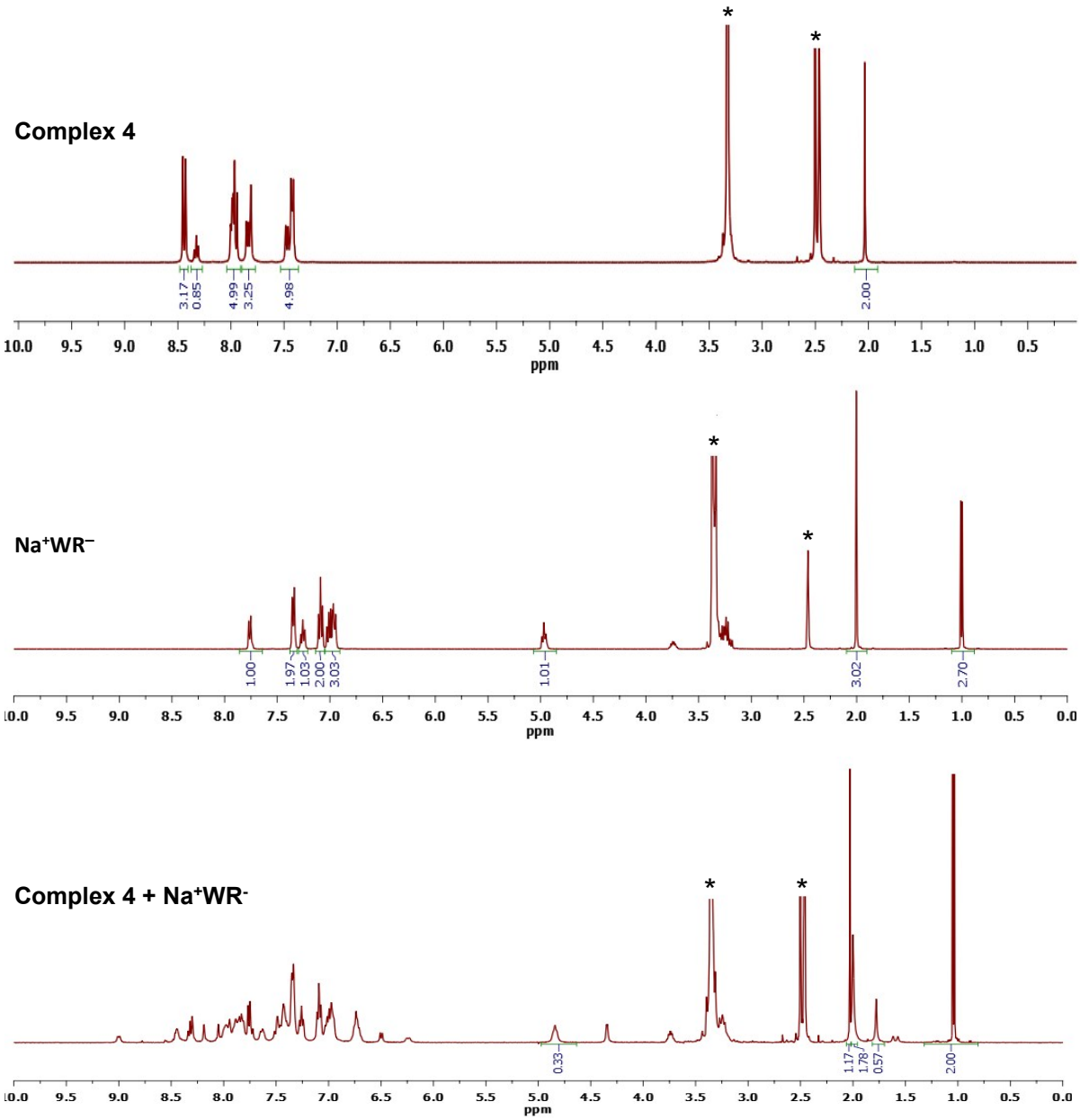

Figure S25. ^{1}H NMR spectra of complex **4**, $Na^{+}WR^{-}$ and complex **4** + $Na^{+}WR^{-}$ in DMSO-d_6 where * represents the residual solvent and/or adventitious water peak(s).

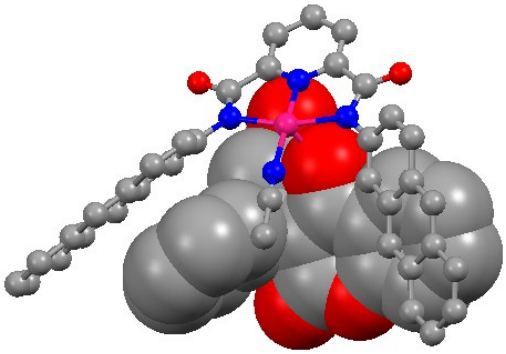

Figure S26. Ball-and-stick representation of docked structure of complex **4** with WR (shown in a space-fill representation).

Table S1. Stern-Volmer Constants (K_{SV}), Detection Limits (DL) and binding Constants (K_b) for Na^+WR^- with palladium complexes **1-4.**

	CH_3CN			HEPES buffer (10 mM, *p*H = 7.4)		
Species	**K_{SV} (M^{-1})**	**DL (nM)**	**K_b (M^{-1})**	**K_{SV} (M^{-1})**	**DL (μM)**	**K_b (M^{-1})**
1 + Na^+WR^-	2.92 x 10^6	3.18	5.48 x 10^5	2.60 x 10^4	0.35	0.109 x 10^5
2 + Na^+WR^-	2.58 x 10^6	3.25	4.84 x 10^5	0.58 x 10^4	0.72	0.042 x 10^5
3 + Na^+WR^-	3.18 x 10^6	3.14	5.69 x 10^5	5.19 x 10^4	0.30	0.212 x 10^5
4 + Na^+WR^-	2.47 x 10^6	3.11	6.38 x 10^5	5.52 x 10^4	0.29	0.282 x 10^5

Table S2. Crystallographic data collection and structure solution parameters for complex **4**.

Empirical Formula	$C_{37}H_{24}N_4O_2Pd$
Formula weight	663.00
T (K)	293(2)
System	Monoclinic
Space group	$P2_1/c$
a (Å)	9.875(5)
b (Å)	30.125(5)
c (Å)	20.458(5)
α (°)	90
β (°)	91.168(5)
γ (°)	90
V (Å^3)	6085(4)
Z	8
ρ_{calc} (mg/m^3)	1.447
F (000)	2688.0
Goodness-of-fit (GOF) on F^2	1.024
Final *R* indices [$I > 2\sigma(I)$]	R_1= 0.1018, wR_2= 0.1768
R indices (all data)	R_1= 0.2203, wR_2= 0.2234
CCDC No.	1522061